ACTA IMEKO
ISSN: 2221-870X
December 2020, Volume 9, Number 4, 106 - 113

Precise Takagi-Sugeno fuzzy logic system for UAV longitudinal stability: an Industry 4.0 case study for aerospace

Enrico Petritoli[1], Fabio Leccese[1]

[1] *Science Department, Università degli Studi 'Roma Tre' Via Della Vasca Navale n°84, 00146, Rome, Italy*

ABSTRACT
Industry 4.0 is making inroads even into the field of aerospace, which is extremely conservative due to the safety concerns involved with the introduction of new technology. We used fuzzy logic to create a very reliable simplification and reduce the complexity of the critical longitudinal stability equations for a flying wing drone. Our approximate method allowed us to have a very light calculation effort at the price of a negligible error in terms of the size and dynamics of the craft, thus reducing the work required by the telecommunication segment that manages the takeoff and landing manoeuvres.

Section: RESEARCH PAPER

Keywords: Precision; Takagi-Sugeno; fuzzy logic; UAV; stability; aerospace

Citation: Enrico Petritoli, Fabio Leccese, Precise Takagi-Sugeno fuzzy logic system for UAV longitudinal stability: an Industry 4.0 case study for aerospace, Acta IMEKO, vol. 9, no. 4, article 14, December 2020, identifier: IMEKO-ACTA-09 (2020)-04-14

Section Editor: Francesco Bonavolonta, University of Naples Federico II, Italy

Received October 14, 2019; **In final form** February 4, 2020; **Published** December 2020

Corresponding author: Fabio Leccese, e-mail: fabio.leccese@uniroma3.it

1. INTRODUCTION

The authors have been involved in the development of a fixed wing tailless drone (UAV). We will examine the critical challenge of maintaining longitudinal stability that confronts aircraft with this design [1]-[3].

In the next sections, we will briefly illustrate the type of hardware that was chosen, and, after discussing the aerodynamic challenges, we will address the fuzzy logic resolution method that was used to simplify the calculations. In the current context of flight in which the ground, air and space segments must converse with each other, the ground segment, thanks to Internet-of-Things (IoT) and Wi-Fi technology, is taking on an increasingly important role for UAVs during flight phases and landing via the base station [4].

We can therefore say that Industry 4.0 is making inroads even into the extremely conservative and slow-to-change field of aerospace. This reluctance to change is, of course, due to a key aspect of both air and spaceflight: safety. It took decades of testing and certification to entrust an airliner to the autopilot, and even now, the cabin must be staffed by a human pilot. Contrary to popular belief, safety is not less important in drones, even though there are no people on board. In the case examined in this paper, we entrust the control of longitudinal stability to an automatic system that, far from behaving like a simple machine, uses fuzzy logic to approach human behaviour, while still avoiding human weaknesses [5].

1.1. State of the Art

The flying wing design (i.e. an aircraft without horizontal empennage) was among the first to appear in the world of aviation; however, it was soon found to be intrinsically unstable. This instability leads to a loss of control if the flight is disturbed by a gust or a manoeuvre. Following the rapid development of aeronautical engineering in the early 1900s, the idea of tailless

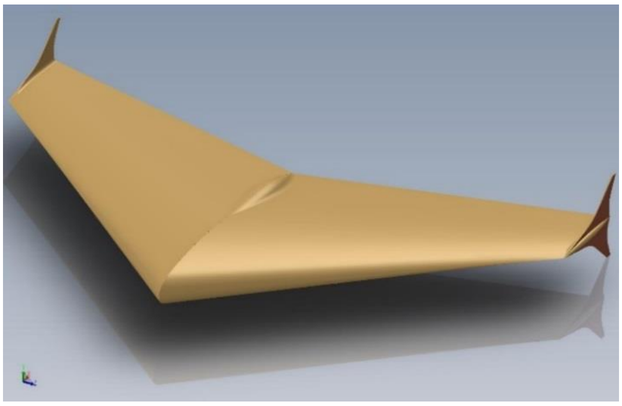

Figure 1. Rendering of the flying wing drone.

aircraft took hold in the world of gliders. In particular, the Horten brothers developed an entire family of gliders of this type. This led to the study and use of special aerofoils optimised for this type of vehicle. After an uncertain start in the 1950s by Northrop Aviation (today Northrop-Grumman), the B-2 *Spirit* arrived in the late 1990s, an aerodynamically mature aircraft from all points of view. In the design of UAVs, the tailless formula was immediately successful, generating a series of models and strategies of use. Generally, they are engaged in missions in which acrobatics are clearly not the main requirement; indeed, stability is an essential feature in their use as aerial photogrammetric platforms. Due to the low drag, as has been noted, they are especially useful for surveillance tasks in temporally demanding missions. For this reason, the use of remote piloting is increasingly abandoned in favour of more tactical-operational autonomy. As a result, autonomous navigation systems that contain robust stability routines have been developed. Within this context, our work is aimed at proposing increasingly fast and efficient calculation methods.

2. THE SYTEM

2.1. The UAV

The design (see Figure 1) of the drone is based on a flying wing: it is tailless with winglets at the wing tips and is energised by a pusher propeller. Such designs have extremely low aerodynamic inducted resistance at the price of a strong criticality: poor longitudinal stability [6]-[8].

In order for the drone to be stable, it is necessary to manage the weight so that the centre of gravity is set lower than in a classically designed aircraft. Furthermore, there is always the danger that it can enter an uncontrollable aerodynamic state outside the flight envelope and fall into a 'dead leaf' condition, which is completely uncontrollable and inevitably leads to the loss of the drone [9]-[11].

2.2. The Flight Control System (FCS)

The Flight Control System (FCS) is the heart of the navigation system: it manages the attitude of the craft, the data coming from the payload and all communications. In order to develop a fast processor for the FCS, our attention was focused immediately on two main problems: firstly, we needed to calculate large volumes of parallel data with a single device; and secondly, we needed an accurate evaluation of approximated stability functions in order to increase the calculation speed.

As stated, the main tasks of the FCS are three: housekeeping (attitude control), data handling from the payload and telecommunications management. The innovation consists in not using three separate microprocessors for all functions but instead wrapping them all into one positively reprogrammable microprocessor.

2.3. The IoT system

In this section, we will examine UAV navigation within the IoT network (see Figure 2).

The UAV receives position signals from the Global Navigation Satellite System (GNSS) constellation, processes them for navigation and then uses telemetry to transmit data to the tracking system [12].

The tracking system consists of a high gain antenna (used to extend the range) that collects the signals and sends them to the server. The server has the task of managing and sorting the signals and sending them to the operator [13].

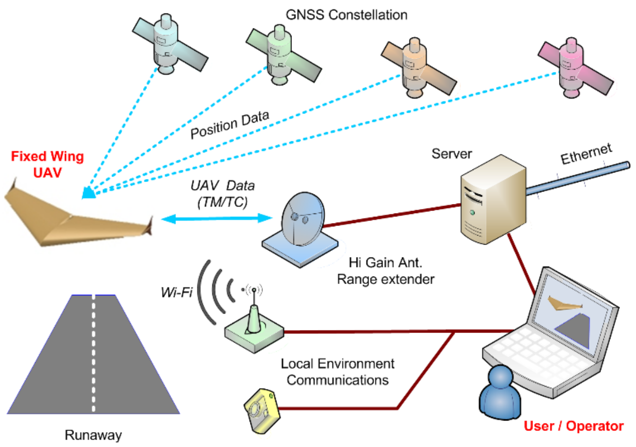

Figure 2. Schematic diagram of the IoT network for UAV general control.

On the landing strip, meanwhile, equipment is available that uses a camera to detect the state of the track and meteorological information, which will then be transmitted via Wi-Fi to the aircraft as it approaches the runway [14].

The advantage of this system is clear: non-essential flight data are not transmitted, keeping the communication systems clear. In Europe, the IEEE 802.15.2 standard assigns the frequency of 868.3 MHz to Telemetry and Telecommands (TTC) for UAV. Since the communication channel is limited, saturating it is extremely easy, regardless of the type of modulation chosen [15].

2.4. Fuzzy Systems

Currently, fuzzy logic-based systems are among the most important applications of fuzzy logic in soft computing and applied mathematics, and they are widely used for solving control problems in all aspects of engineering [16]-[21]. The popularity of fuzzy logic-based systems is due to their ability to appropriately simulate human thinking, surpassing the limits of Boolean logic and expressing the system in its full complexity. The Takagi-Sugeno model (T-S), represented by the fuzzy relation 'IF-THEN', manages to describe a non-linear dynamic system with a linearised model that meets all the conditions set and has a negligible error rate that will be shown at the end of the paper [22]-[27]. The logical processes that lead to the formulation of the inference conditions are as follows: firstly, the logical process must undergo *fuzzification*, a modelling based on the rigorous application of fuzzy (not Boolean) rules; and finally, the whole linear system must be *defuzzified* to return to the physical world [28].

2.5. Fuzzy Systems Algebra

For clarity of exposition, we will briefly introduce the fuzzy algebra method that we used [29]-[34].

Consider a fuzzy set Φ_{ij} composed of:

$$\begin{cases} \mathbb{z}_1(t) = \Phi_{i1} \\ \mathbb{z}_2(t) = \Phi_{i2} \\ \mathbb{z}_3(t) = \Phi_{i3} \\ \dots\dots\dots \\ \mathbb{z}_{p-1}(t) = \Phi_{i(p-1)} \\ \mathbb{z}_p(t) = \Phi_{ip} \end{cases} \tag{1}$$

For the model rule, i^{th}, we have a set of r model rules, and then we have:

$\zeta_v(t)$ = input vector

$x_v(t)$ = state vector

$\xi_v(t)$ = output vector

The complete rule now is:

$$\text{IF } \langle z_1(t) = \Phi_{i1} \text{ AND } \mathbb{z}_2(t) = \Phi_{i2} \text{ AND } \ldots \text{ AND } \mathbb{z}_p(t) = \Phi_{ip} \rangle \tag{2}$$

$$\text{THEN } \begin{cases} x_v(t+1) = \mathcal{A}_i x_v(t) + \mathcal{B}_i \zeta_v(t) \\ y(t) = \mathcal{C}_i x_v(t) \end{cases} \tag{3}$$

with $i = 1,2, \ldots r$

where

$$\mathcal{A}_i = \begin{pmatrix} \mathbb{g}_{11} & \cdots & \mathbb{g}_{p1} \\ \vdots & \ddots & \vdots \\ \mathbb{g}_{1p} & \cdots & \mathbb{g}_{pp} \end{pmatrix}. \tag{4}$$

$\mathcal{A}_i$: is the matrix (square) with the real elements and $\mathbb{z}_1(t), \mathbb{z}_2(t), \ldots, \mathbb{z}_p(t)$ are known premise variables.

Each subsystem is represented by a linear equation:

$$\mathcal{A}_i x_v(t) + \mathcal{B}_i \zeta_v(t)\,. \tag{5}$$

Now for the model we have:

$$x_v(t+1) = \frac{\sum_{i=1}^{r} \varsigma_i[\mathbb{z}(t)]\{\mathcal{A}_i x(t) + \mathcal{B}_i \zeta_v(t)\}}{\sum_{i=1}^{r} \varsigma_i[\mathbb{z}(t)]}. \tag{6}$$

Simplifying:

$$x_v(t+1) = \sum_{i=1}^{r} h_i[\mathbb{z}(t)]\{\mathcal{A}_i x(t) + \mathcal{B}_i \zeta_v(t)\}\,. \tag{7}$$

So, according to (6)

$$\xi_v(t) = \frac{\sum_{i=1}^{r} \varsigma_i[\mathbb{z}(t)]\mathcal{C}_i x(t)}{\sum_{i=1}^{r} \varsigma_i[\mathbb{z}(t)]}. \tag{8}$$

Then we have:

$$\xi_v(t) = \sum_{i=1}^{r} h_i[\mathbb{z}(t)]\,\mathcal{C}_i x(t) \tag{9}$$

where

$$\mathbb{z}(t) = \left[\mathbb{z}_1(t) \cdot \mathbb{z}_2(t) \cdot \ldots\ldots\ldots\ldots \cdot \mathbb{z}_p(t)\right]. \tag{10}$$

The expression of ς_i is:

$$\varsigma_i[\mathbb{z}(t)] = \prod_{j=1}^{p} \Phi_{ij}\left[\mathbb{z}_j(t)\right]. \tag{11}$$

Then:

$$h_i[\mathbb{z}(t)] = \frac{\varsigma_i[\mathbb{z}(t)]}{\sum_{i=1}^{r} \varsigma_i[\mathbb{z}(t)]}. \tag{12}$$

The membership of $\mathbb{z}_j(t)$ in Φ_{ij} is:

$$\begin{cases} \sum_{i=1}^{r} \varsigma_i[\mathbb{z}(t)] > 0 \\ \varsigma_i[\mathbb{z}(t)] \geq 0, \text{with } i = 1,2, \ldots r\,. \end{cases} \tag{13}$$

We have

$$\begin{cases} \sum_{i=1}^{r} h_i[\mathbb{z}(t)] = 1 \\ h_i[\mathbb{z}(t)] \geq 0, \text{with } i = 1,2, \ldots r \end{cases} \tag{14}$$

for all *t*.

3. FUZZY STABILITY

3.1. Fuzzy Model Application

For the longitudinal stability interval of the drone, we now have the following system:

$$\begin{cases} \dot{x}_V = v \\ L_\mathrm{w} \cong \frac{1}{2}\, v^2\, \mathbb{F}\, \alpha_\mathrm{w} \end{cases} \tag{15}$$

where

$$v_\mathrm{min} < v \leq v_\mathrm{max} \tag{16}$$

v_min = minimum allowed speed ($= v_\mathrm{stall}$)

v_max = maximum allowed speed according to the linearity interval.

So (15) becomes:

$$\begin{bmatrix} x_1 \\ x_2 \end{bmatrix} = \begin{bmatrix} \dot{x}_V \\ L_\mathrm{w} \end{bmatrix} = \begin{bmatrix} 1 & 0 \\ v\, \mathbb{F}\, \alpha_\mathrm{w} & \frac{1}{2}\, v^2\, \mathbb{F} \end{bmatrix} \cdot \begin{bmatrix} v \\ \alpha_\mathrm{w} \end{bmatrix}. \tag{17}$$

The fuzzy variables v and α_w are nonlinear terms in the expressions.

Posing z_1 and z_2 as premise variables that may be functions of state variables,

$$\begin{bmatrix} z_1 \\ z_2 \end{bmatrix} = \begin{bmatrix} v\, \mathbb{F}\, \alpha_w \\ \frac{1}{2}\, v^2\, \mathbb{F} \end{bmatrix} \tag{18}$$

we can express (17) as:

$$\begin{bmatrix} 1 & 0 \\ v\, \mathbb{F}\, \alpha_\mathrm{w} & \frac{1}{2}\, v^2\, \mathbb{F} \end{bmatrix} = \begin{bmatrix} 1 & 0 \\ z_1 & z_2 \end{bmatrix}. \tag{19}$$

Now we should calculate the minimum and maximum of the parameters:

$$\begin{cases} v \in [v_\mathrm{stall} \quad v_\mathrm{max}] \\ \alpha_\mathrm{w} \in [-4 \quad 8]\,, \text{in } ^\circ. \end{cases} \tag{20}$$

Therefore, expanding (19), we have the limits:

$$\begin{cases} \max\limits_{v, \alpha_\mathrm{w}} z_1 = 8\, v_\mathrm{max}\, \mathbb{F} \\ \min\limits_{v, \alpha_\mathrm{w}} z_1 = -4\, v_\mathrm{stall}\, \mathbb{F} \\ \max\limits_{v, \alpha_\mathrm{w}} z_2 = \frac{1}{2} {v_\mathrm{max}}^2\, \mathbb{F} \\ \min\limits_{v, \alpha_\mathrm{w}} z_2 = \frac{1}{2} {v_\mathrm{stall}}^2\, \mathbb{F}\,. \end{cases} \tag{21}$$

Therefore v and α_w can be represented by membership functions M_1, M_2, N_1 and N_2 as follows:

$$z_1 = \mathrm{M}_1(z_1) \cdot (8\, v_\mathrm{max}\, \mathbb{F}) + \mathrm{M}_2(z_1) \cdot (-4\, v_\mathrm{stall}\, \mathbb{F}) \tag{22}$$

$$z_2 = \mathrm{N}_1(z_2) \cdot \left(\frac{1}{2}\, {v_\mathrm{max}}^2\, \mathbb{F}\right) + \mathrm{N}_2(z_2) \cdot \left(\frac{1}{2}\, {v_\mathrm{stall}}^2\, \mathbb{F}\right) \tag{23}$$

where

$$\begin{cases} M_1(z_1) + M_2(z_1) = 1 \\ N_1(z_2) + N_2(z_2) = 1 \end{cases} \quad (24)$$

Now we introduce the model rule. This is the *liaison* between real physical elements and the limits.

#1: IF z_1 is 'high' AND z_2 is 'big' THEN $\dot{x}_V = A_1 \cdot x_V$
#2: IF z_1 is 'high' AND z_2 is 'small' THEN $\dot{x}_V = A_2 \cdot x_V$
#3: IF z_1 is 'low' AND z_2 is 'big' THEN $\dot{x}_V = A_3 \cdot x_V$
#4: IF z_1 is 'low' AND z_2 is 'small' THEN $\dot{x}_V = A_4 \cdot x_V$

where for the A_n parameter we have:

$$A_1 = \begin{bmatrix} 1 & 0 \\ \max z_1 & \max z_2 \\ z_1 \in high & z_2 \in big \end{bmatrix} = \begin{bmatrix} 1 & 0 \\ 8\, v_{\max}\, \mathbb{F} & \frac{1}{2} v_{\max}{}^2 \mathbb{F} \end{bmatrix} \quad (25)$$

$$A_2 = \begin{bmatrix} 1 & 0 \\ \max z_1 & \max z_2 \\ z_1 \in high & z_2 \in small \end{bmatrix} = \begin{bmatrix} 1 & 0 \\ 8\, \rho\, v_{\max}\, \mathbb{F} & \frac{1}{2} v_{\mathrm{stall}}{}^2\, \mathbb{F} \end{bmatrix} \quad (26)$$

$$A_3 = \begin{bmatrix} 1 & 0 \\ \max z_1 & \max z_2 \\ z_1 \in low & z_{12} \in big \end{bmatrix} = \begin{bmatrix} 1 & 0 \\ -4\, \rho\, v_{\mathrm{stall}}\, \mathbb{F} & \frac{1}{2}\, v_{\max}{}^2\, \mathbb{F} \end{bmatrix} \quad (27)$$

$$A_4 = \begin{bmatrix} 1 & 0 \\ \max z_1 & \max z_2 \\ z_1 \in low & z_{12} \in small \end{bmatrix} = \begin{bmatrix} 1 & 0 \\ -4\, v_{\mathrm{stall}}\, \mathbb{F} & \frac{1}{2}\, v_{\mathrm{stall}}{}^2\, \mathbb{F} \end{bmatrix} \quad (28)$$

Now, $\dot{x}_V$ can be derived from the *defuzzification* process as:

$$\dot{x}_V = h_1(z)\, A_1 \cdot x_v + h_2(z)\, A_2 \cdot x_V + h_3(z)\, A_3 \cdot x_{MV} + h_4(z)\, A_4 \cdot x_V \quad (29)$$

in which

$$\begin{cases} h_1(z) = M_1(z_1) \times N_1(z_2) \\ h_2(z) = M_1(z_1) \times N_2(z_2) \\ h_3(z) = M_2(z_1) \times N_1(z_2) \\ h_4(z) = M_2(z_1) \times N_2(z_2) \end{cases} \quad (30)$$

This fuzzy model exactly represents the nonlinear system in the region $[v_{\mathrm{stall}} \quad v_{\max}] \times [-4° \quad 8°]$ in the v, α_w space.

As is evident in equations (29) and (30), the responses of the fuzzy model can exactly follow the responses of the original equations, which means the fuzzy model can exactly represent the original system in the pre-specified domains. That is to say, inside of the boundaries of v and α_w, the above approach can accurately represent the original system. The advantage of this method is immediate: the calculation effort is enormously decreased. In practice, everything is resolved through linear systems or simple multiplication between square matrices.

3.2. The simulation

The simulation was performed with the combined Matlab®/ Simulink® tool, and the results were validated separately on a sample of 44 specific points.

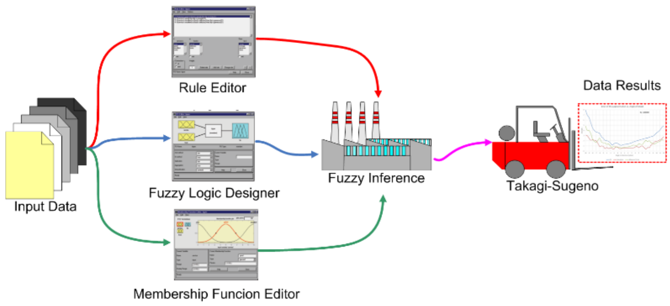

Figure 3. *Fuzzification* process.

The difference between a classical solution and a fuzzy one is simple: a classical set contains elements that satisfy precise properties of membership, while a fuzzy set contains elements that satisfy imprecise properties of membership. Figure 3 illustrates the *fuzzification* procedure for the problem, which may be defined as transforming the available data from a crisp set into a fuzzy set. Basically, this operation translates accurate crisp input values into linguistic variables. For this, it is necessary to define the rules, the membership functions and the architecture. Subsequently, thanks to the T-S method (as explained above), a mathematical result is reached.

Figure 4 illustrates the data evaluation process. Initially, a rather large set of real data obtained from tests on real drones (about 13 Gb) was produced. These were processed in parallel both with the fuzzy method and with the system method of equations. Since we knew the solution, we could therefore establish the percentage of error introduced in each method. Obviously and as expected, the second provides less approximate data but requires much more calculation. To determine the difference, each solution was associated with a marker providing the calculation time. At the end of the process, we added up the time data and found that, on average, the T-S method reduced calculation time by 83.7 % for each cycle, thus allowing for much faster physical feedback. This speed is paid for with greater error, as we will see in the next paragraph, but the error is always within an absolutely acceptable range for our navigation system.

3.3. The error

Figure 5 shows the results of our work, with the blue line representing the percentage error of the approximate solution. Takagi-Sugeno is traced with respect to the 'exact' solution that was calculated with recursive and time-consuming numerical methods. For completeness, we have also included the generated simulation of the completed aircraft (red line). The green line indicates the difference between the two. The excellent behaviour of the T-S approximation within the linearity interval

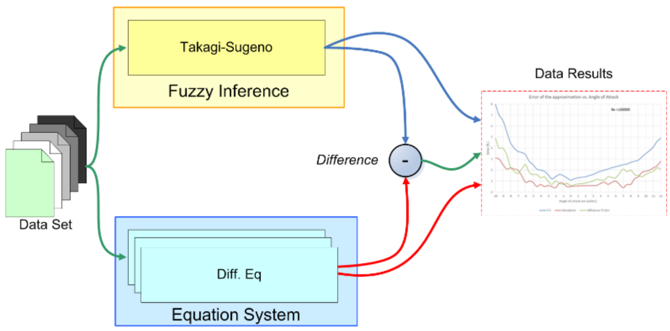

Figure 4. Simulation block architecture.

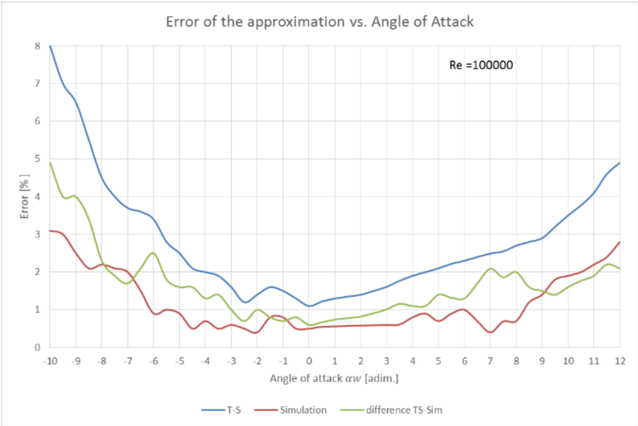

Figure 5. Error vs. angle of attack. The T-S solution is blue, the total simulation is red and the difference is green.

$-4° \leq \alpha_w < 8°$ is immediately visible, although it decays rapidly outside this non-linear characteristic.

4. CONCLUSIONS

In a more dynamic context, the execution speed of the algorithms as well as the structure or shape of drones helps to make some critical manoeuvring phases more agile by drastically reducing the computational cost of the analysis (see Figure 5). For this reason, we feel our work is justified.

The drone used in our case study was a fixed-wing UAV that required micro-tapping of all ancillary and non-viable systems. Fuzzy logic was used to reduce the complexity of the longitudinal stability equations, which are critical for flying wings, and thus reduce the computational load on the FCS.

Our approximate calculation method allowed us to have a very light calculation effort at the price of a negligible error in terms of the size and dynamics of the craft.

APPENDIX A: The Horten Aerofoil

We chose the Horten ($t/c = 11$ %, $f/c = 2$ %) non-symmetrical aerofoil. It behaves quite well aerodynamically in the expected speed range, with a stall preceded by buffeting at a reasonably low stall speed (see Figure 6a and 6b).

In order to move the aerodynamic centre backwards, a 30-degree sweep angle was chosen, resulting in a CG that was not too far forward but provided a noticeable decrease in drag [35]. For reference, we will consider the aerofoil to which the lift force of the wing is applied (ideally). This aerofoil was originally designed and used by the Horten brothers, who built a number of high-performance sailplanes during the 1930s and 1940s. Their designs are legendary, although some of their published performance data are a little bit too good [36].

Their planes were well known for their good handling characteristics, which could be of greater importance than the actual performance figures from our project [37].

A.1 The Longitudinal Stability

For the balance of the forces around the Y-axis we have (see Figure 7):

$$\begin{aligned} M_{\mathrm{cg_w}} = {} & L_\mathrm{w}\cos(\alpha_\mathrm{w}-i_\mathrm{w})\cdot(x_\mathrm{cg}-x_\mathrm{ac}) \\ & + D_\mathrm{w}\sin(\alpha_\mathrm{w}-i_\mathrm{w})\cdot(x_\mathrm{cg}-x_\mathrm{ac}) \\ & + L_\mathrm{w}\sin(\alpha_\mathrm{w}-i_\mathrm{w})\cdot(z_\mathrm{cg}-z_\mathrm{ac}) \\ & + (-D_\mathrm{w})(\alpha_\mathrm{w}-i_\mathrm{w})\cdot(z_\mathrm{cg}-z_\mathrm{ac}) + M_{\mathrm{ac_w}} \end{aligned} \tag{31}$$

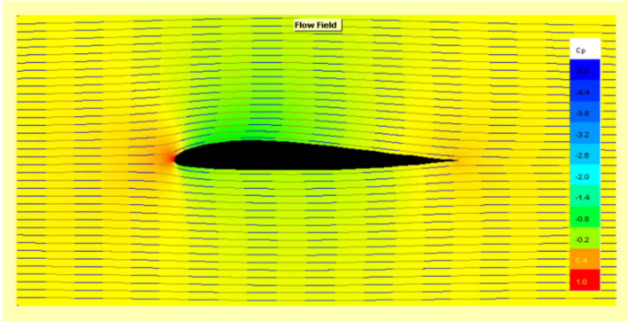

a)

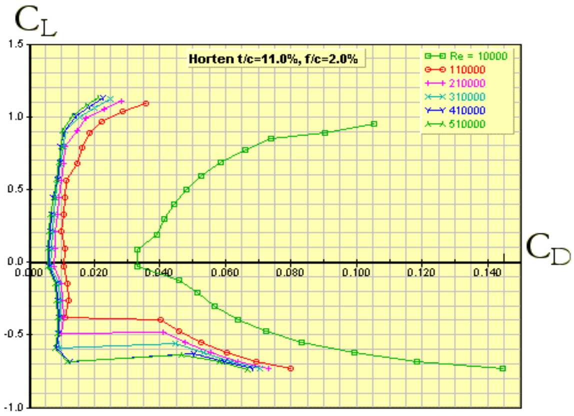

b)

Figure 6. Horten (t/c = 11 %, f/c = 2 %) aerofoil a) flow field and pressure gradient of conditions: *Speed* = 60 km/h, $Re = 10^5$ and $\alpha_\mathrm{w} = 0°$ and b) C_L vs. C_D behaviour.

where

$M_{\mathrm{cg_w}}$ = moment of all the wing forces around the centre of gravity

L_w = lift force of the wing

D_w = drag force of the wing

α_w = angle between the main chord and the wind direction (angle of attack)

i_w = angle between the main chord and the X-axis

x_cg = distance of centre of gravity from the Z-axis

x_ac = distance of aerodynamic centre of gravity from the Z-axis

z_cg = distance of centre of gravity from the X-axis

z_ac = distance of aerodynamic centre from the X-axis

$M_{\mathrm{ac_w}}$ = moment of all the wing forces around the aerodynamic centre

C. G. = centre of gravity

A. C. = aerodynamic centre

Now we consider that if the angle of attack is reasonably small, the lift is much less than the drag:

$$L_\mathrm{w} \gg D_\mathrm{w} \tag{32}$$

and for small angles:

$$\alpha_\mathrm{w} - i_\mathrm{w} \ll 1 \tag{33}$$

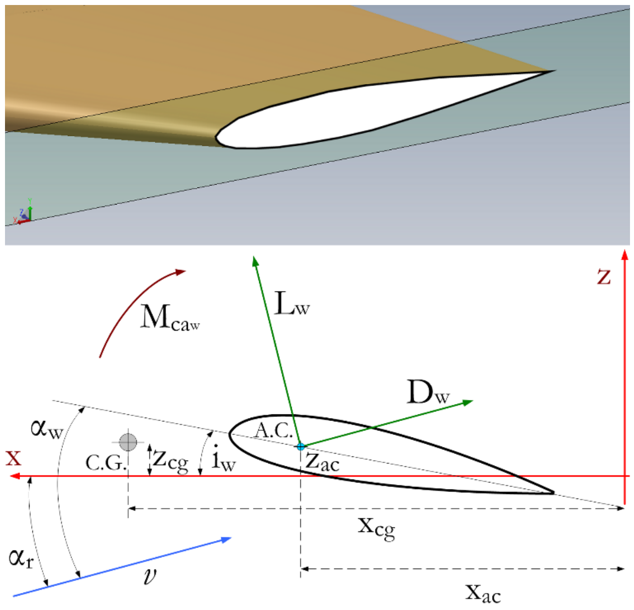

Figure 7. Force balance around the Y-axis.

So we have:

$$\sin(\alpha_{\mathrm{w}} - i_{\mathrm{w}}) \approx 0 \tag{34}$$

and

$$\cos(\alpha_{\mathrm{w}} - i_{\mathrm{w}}) \ll 1\,. \tag{35}$$

For thin aerofoils and small angles, we have:

$$z_{\mathrm{cg}} = z_{\mathrm{ac}} \approx 0 \tag{36}$$

so equation (31) becomes

$$M_{\mathrm{cg_w}} = L_{\mathrm{w}} \cdot (x_{\mathrm{cg}} - x_{\mathrm{ac}}) + M_{\mathrm{ac_w}}\,. \tag{37}$$

and the new stability conditions are:

$$M_{\mathrm{cg_w}} - M_{\mathrm{ac_w}} = L_{\mathrm{w}} \cdot (x_{\mathrm{cg}} - x_{\mathrm{ac}})\,. \tag{38}$$

So

$$L_{\mathrm{w}} = \frac{M_{\mathrm{cg_w}} - M_{\mathrm{ac_w}}}{x_{\mathrm{cg}} - x_{\mathrm{ac}}}\,. \tag{39}$$

This equation represents the longitudinal stability of the craft.

Now we consider the C_L vs. a_w characteristics of the aerofoil. The expression for the lift L is:

$$L_{\mathrm{w}} = \frac{1}{2}\,\rho\, v^2\, S\, C_L\,. \tag{40}$$

Applying this to (39), we have:

$$\frac{1}{2}\,\rho\, v^2\, S\, C_L = \frac{M_{\mathrm{cg_w}} - M_{\mathrm{ac_w}}}{x_{\mathrm{cg}} - x_{\mathrm{ac}}} \tag{41}$$

where

ρ = air density

S = wing surface

v = relative speed (in reference to the air)

C_L = coefficient of lift

For the Horten aerofoil, according to the characteristic C_L vs. α_{w}, the angle of attack in the interval [-4 °; +10 °], is linear (see the red zone of Figure 8).

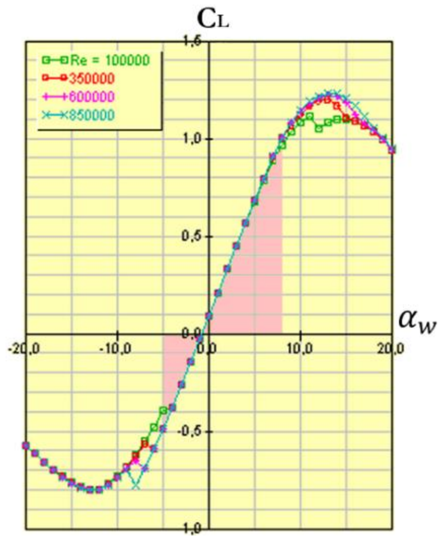

Figure 8. Horten (t/c = 11 %, f/c = 2 %) aerofoil C_L vs. α_w characteristics ($Re = 10^5$ - 8.5×10^5): the linear interval is evidenced in red.

We can linearise equation (40), and we have:

$$L_{\mathrm{w}} = \frac{1}{2}\,\rho\, v^2\, S\, k\, \alpha_{\mathrm{w}}\,. \tag{42}$$

Posing:

$$\mathbb{F} = \rho\, k\, S \tag{43}$$

we have:

$$L_{\mathrm{w}} = \frac{1}{2}\, v^2\, \mathbb{F}\, \alpha_{\mathrm{w}}\,. \tag{44}$$

This is the equation set considered in paragraph 3.1.

REFERENCES

[1] R. Abdelkrim, H. Gassara, M. Chaabane, A. El Hajjaji, Stability approaches for Takagi-Sugeno systems, 2015 IEEE International Conference on Fuzzy Systems (FUZZ-IEEE), Istanbul, Turkey, 2015, pp. 1-6.
DOI: https://doi.org/10.1109/FUZZ-IEEE.2015.7338051

[2] R. Robles, M. Bernal, Comments on "Exact output regulation for nonlinear systems described by Takagi–Sugeno fuzzy models", IEEE Transactions on Fuzzy Systems, 23 no. 1 (2015), pp. 230-233.
DOI: https://doi.org/10.1109/TFUZZ.2014.2321773

[3] F. Leccese, M. Cagnetti, S. Giarnetti, E. Petritoli, I. Luisetto, S. Tuti, R. Durovic-Pejcev, T. Dordevic, A. Tomašević, V. Bursić, V. Arenella, P. Gabriele, A. Pecora, L. Maiolo, E. De Francesco, G. Schirripa Spagnolo, R. Quadarella, L. Bozzi, C. Formisano, A simple Takagi-Sugeno fuzzy modelling case study for an underwater glider control system, 2018 IEEE International Workshop on Metrology for the Sea: Learning to Measure Sea Health Parameters, MetroSea 2018, Bari, Italy, 8-10 October 2018, pp. 262-267.
DOI: https://doi.org/10.1109/MetroSea.2018.8657877

[4] W. Jamel, A. Khedher, N. Bouguila, K. Ben Othman, Design of unknown inputs and multiple integral observers for Takagi-Sugeno multiple model, 2015 IEEE 12th International Multi-Conference on Systems, Signals & Devices (SSD15), Mahdia, Tunisia, 2015, pp. 1-6.
DOI: https://doi.org/10.1109/SSD.2015.7348194

[5] J. Mendes, F. Souza, R. Araújo, Online evolving fuzzy control design: An application to a CSTR plant, 2017 IEEE 15th International Conference on Industrial Informatics (INDIN),

Emden, Germany, 2017, pp. 218-225.
DOI: https://doi.org/10.1109/INDIN.2017.8104774
[6] J. M. Buffington, A. G. Sparks, Comparison of dynamic inversion and LPV tailless flight control law designs, Proceedings of the 1998 American Control Conference. ACC (IEEE Cat. No.98CH36207), Philadelphia, PA, USA, 1998, Vol.2 pp. 1145-1149.
DOI https://doi.org/10.1109/ACC.1998.703591
[7] Y. Fan, J. Zhu, J. Zhu, Z. Sun, Modeling and simulation research on tailless unmanned aerial vehicle, The Proceedings of the Multiconference on "Computational Engineering in Systems Applications", Beijing, China, 2006, pp. 640-645.
DOI: https://doi.org/10.1109/CESA.2006.4281731
[8] A. D. Ngo, W. C. Reigelsperger, S. S. Banda, J. A. Bessolo, Tailless aircraft control law design using dynamic inversion & synthesis, Proceeding of the 1996 IEEE International Conference on Control Applications held together with IEEE International Symposium on Intelligent Control, Dearborn, MI, USA, 1996, pp. 107-112.
DOI: https://doi.org/10.1109/CCA.1996.558615
[9] J. D. Boskovic, Sai-Ming Li, R. K. Mehra, Study of an adaptive reconfigurable control scheme for tailless advanced fighter aircraft (TAFA) in the presence of wing damage, IEEE 2000. Position Location and Navigation Symposium (Cat. No.00CH37062), San Diego, CA, USA, 2000, pp. 341-348.
DOI: https://doi.org/10.1109/PLANS.2000.838323
[10] N. G. M. Rademakers, R. Akmeliawati, R. Hill, C. Bil, H. Nijmeijer, Modelling and gain scheduled control of a tailless fighter, 5th Asian Control Conference (IEEE Cat. No.04EX904), Melbourne, Victoria, Australia, 20-23 July 2004, Vol.1 pp. 374-382.
DOI: https://doi.org/10.1109/ASCC.2004.184792
[11] V. V. Patel, C. Cao, N. Hovakimyan, K. A. Wise, E. Lavretsky, L1 Adaptive controller for tailless unstable aircraft, 2007 American Control Conference, New York, NY, USA, 2007, pp. 5272-5277.
DOI: https://doi.org/10.1109/ACC.2007.4283114
[12] J. D. Boskovic, Sai-Ming Li, R. K. Mehra, Reconfigurable flight control design using multiple switching controllers and online estimation of damage-related parameters, Proceedings of the 2000 IEEE International Conference on Control Applications. Conference Proceedings (Cat. No.00CH37162), Anchorage, AK, USA, 2000, pp. 479-484.
DOI: https://doi.org/10.1109/CCA.2000.897470
[13] J. S. R. Jang, ANFIS: adaptive network-based fuzzy inference systems, IEEE Transactions on Systems Man and Cybernetics 23 (1993), pp. 665-685.
DOI: https://doi.org/10.1109/21.256541
[14] H. Zhang, C. Dang, J. Zhang, Decentralized fuzzy filtering for nonlinear interconnected systems with multiple time delays, IEEE Transactions on Systems Man and Cybernetics Part B: Cybernetics 40 (2010), pp. 1197-1203.
DOI: https://doi.org/10.1109/TSMCB.2010.2042956
[15] P. P. Angelov, R. A. Buswell, V. I. Hanby, J. A. Wright, Automatic generation of fuzzy rule-based models from data by genetic algorithms, in: Advances in Soft Computing. R. John, R. Birkenhead (editors). Physica, Heidelberg, 2001, ISBN 978-3-7908-1361-6, pp. 31-40.
DOI: https://doi.org/10.1007/978-3-7908-1829-1_4
[16] T. Takagi, M. Sugeno, Fuzzy identification of systems and its applications to modelling and control, IEEE Transactions on Systems, Man, and Cybernetics, SMC-15, 1 (1985), pp. 116-132.
DOI: https://doi.org/10.1109/TSMC.1985.6313399
[17] K. Shimojima, T. Fukuda, Y. Hasegawa, Self-tuning fuzzy modeling with adaptive membership function rules and hierarchical structure based on genetic algorithm, Fuzzy Sets Syst., 71 (1995), pp. 295-309.
DOI: https://doi.org/10.1016/0165-0114(94)00280-K
[18] U. Sandler, L. Tsitolovsky, Neural Cell Behavior and Fuzzy Logic, Springer International Publishing, Boston, 2008, ISBN: 978-0-387-09542-4
[19] R. M. Tong, The construction and evaluation of fuzzy models, in: Advances to Fuzzy Set Theory and Applications. M. M. Gupta (editor). Plenum, New York 1979, ISBN: 0080263335, 9780080261517, pp. 312-355.
[20] I. Kilani, D. Jabri, S. B. H. A. Naoui, M. N. Abdelkrim, An unknown input observer for Takagi Sugeno descriptor system with unmeasurable premise variable, 10th International Multi-Conferences on Systems, Signals & Devices 2013 (SSD13), Hammamet, Tunisia, 2013, pp. 1-5.
DOI: https://doi.org/10.1109/SSD.2013.6564129
[21] A. J. Torabi, M. J. Er, X. Li, B. S. Lim, Sequential fuzzy clustering based dynamic fuzzy neural network for fault diagnosis and prognosis, Neurocomputing, 196 (2016), pp. 31-41.
DOI: http://dx.doi.org/10.1016/j.neucom.2016.02.036
[22] F. A. Haouari, B. Cherki, M. Djemai, Sliding mode observers for Takagi-Sugeno fuzzy models, 3rd International Conference on Systems and Control, Algiers, Algeria, 2013, pp. 1061-1065.
DOI: https://doi.org/10.1109/ICoSC.2013.6750986
[23] Gui-Ju Shi, Kun-Feng Lu, Ji-Qing Qiu, Robust passive control for uncertain Takagi-Sugeno fuzzy neutral systems with mixed time delays, 2009 International Conference on Machine Learning and Cybernetics, Hebei, China, 2009, pp. 800-805.
DOI: https://doi.org/10.1109/ICMLC.2009.5212423
[24] J. Y. Bae, Y. Badr, A. Abraham, A Takagi-Sugeno fuzzy model of a rudimentary angle controller for artillery fire, 2009 11th International Conference on Computer Modelling and Simulation, Cambridge, USA, 2009, pp. 59-64.
DOI: https://doi.org/10.1109/UKSIM.2009.105
[25] R. Raj, B. M. Mohan, Modelling and analysis of a general Takagi-Sugeno fuzzy PI/PD controller with modified rule base, 2016 IEEE Students' Technology Symposium (TechSym), Kharagpur, India, 2016, pp. 169-174.
DOI: https://doi.org/10.1109/TechSym.2016.7872676
[26] Y. Lin, X. Zhou, S. Gu, S. Wang, The Takagi-Sugeno intuitionistic fuzzy systems are universal approximators, 2nd International Conference on Consumer Electronics, Communications and Networks (CECNet), Yichang, China, 2012, pp. 2214-2217.
DOI: https://doi.org/10.1109/CECNet.2012.6202025
[27] M. B. Gorzakzany, J. B. Kiszka, M. S. Stachowicz, Some problems of studying adequacy of fuzzy models, in: Fuzzy Set and Possibility Theory: Recent Developments. R. R. Yager (editor). Pergamon, New York, 1982, ISBN: 0080262945, 9780080262949, pp. 134-136.
[28] K. Crockett, A. Latham, D. Mclean, J. O'Shea, A fuzzy model for predicting learning styles using behavioral cues in an conversational intelligent tutoring system, 2013 IEEE International Conference on Fuzzy Systems (FUZZ), Hyderabad, India, 2013, pp. 1-8.
DOI: https://doi.org/10.1109/FUZZ-IEEE.2013.6622382
[29] P. P. Angelov, D. P. Filev, An approach to online identification of Takagi-Sugeno fuzzy models, IEEE Transactions on Systems, Man, and Cybernetics, Part B (Cybernetics), 34 no. 1 (2004), pp. 484-498.
DOI: https://doi.org/10.1109/TSMCB.2003.817053
[30] M. Abyad, A. Karama, A. Khallouq, Modelling and control of a biological process using the fuzzy logic Takagi -Sugeno, 2017 International Renewable and Sustainable Energy Conference (IRSEC), Tangier, Morocco, 2017, pp. 1-5.
DOI: https://doi.org/10.1109/IRSEC.2017.8477399
[31] S. Guillaum, Designing fuzzy inference systems from data: an interpretability-oriented review, IEEE Trans. Fuzzy Syst., 9 no. 2 (2001), pp. 426-443.
DOI: https://doi.org/10.1109/91.928739
[32] N. Nomura, I. Hayashi, N. Wakami, A self-tuning method of fuzzy control by descent method, in: Fuzzy Logic Theory and Decision Library. R. Lowen, M. Roubens (editors). Springer International Publishing, Dordrecht, 1993, ISBN: 978-94-010-4890-3, pp. 155-158.
[33] W. Zhang, Y. Ren, H. Zhang, Y. Hu, M. Sun, Research on the integrated neural network water inrush repdiction system based on

Takagi-Sugeno fuzzy criteria, 2008 Fourth International Conference on Natural Computation, Jinan, China, 2008, pp. 228-231.
DOI: https://doi.org/10.1109/ICNC.2008.91
[34] W. Guo, Z. Xiu, Output direct feedback control for Takagi-Sugeno fuzzy systems, 6th World Congress on Intelligent Control and Automation, Dalian, China, 2006, pp. 3734-3738.
DOI: https://doi.org/10.1109/WCICA.2006.1713068
[35] F. W. Riegels, Aerofoil Sections, Butterworths & Co. Ltd., London, 1961.
[36] Yomg Fan, J.-H. Zhu, X.-Y. Meng, Kai Liu, X.-L. Yang, Intelligent method based coordinated integrated flight control of a tailless STOVL, 8th World Congress on Intelligent Control and Automation, Jinan, China, 2010, pp. 85-90.
DOI: https://doi.org/10.1109/WCICA.2010.5553863
[37] R. Murray-Smith, T. A. Johanson, Operating regime approach to nonlinear modeling and control, in: Multiple Model Approaches to Modeling and Control. R. Murray-Smith, T. Johanson (editors). Taylor & Francis, UK, ISBN: 0-7484-0595-X, pp. 3-72.